Int. J. Environ. Res., 9(4):1201-1210, Autumn 2015
ISSN: 1735-6865

Recycling of Residual Oil Fly Ash: Synthesis and Characterization of Activated Carbon by Physical Activation Methods for Heavy Metals Adsorption

Salehin, S.[1*], Aburizaiza, A. S.[1,2] and Barakat, M. A.[1,2,3]

[1]Department of Environmental Sciences, Faculty of Meteorology, Environment and Arid Land Agriculture, King Abdulaziz University, Jeddah, 21589, Saudi Arabia
[2]Center of Excellence in Environmental Studies, King Abdulaziz University,Saudi Arabia
[3]Central Metallurgical R & D Institute, Helwan 11421, Cairo, Egypt

Received 11 Nov. 2014; Revised 15 Feb. 2015; Accepted 21 Feb. 2015

ABSTRACT: In this study, the recycling possibility of residual oil fly ash (ROFA) towards preparing activated carbon and its application in environmental remediation through adsorbing Cu (II) and Pb (II) ions from aqueous solutions were investigated. Activated carbons were prepared using two different physical activation methods such as under steam flow at 950 ^{0}C, and combined steam and CO_2 flow at 850 ^{0}C for 2 hours. Characterization of activated carbons was done by BET surface area method, scanning electron microscopy (SEM), Fourier transform infra-red spectroscopy (FTIR), and X-ray diffraction technique (XRD). Combined gasification increased the surface area of ROFA particles quite higher (110.89 to 423.09 m^2/g) than only steam activation (275.07 m^2/g). Development of microporosity was also achieved during the treatments and it increased from 0.043 cc/g (raw ash) to 0.325 in steam activated samples, and 0.078 in combined gas activated samples. FTIR analysis showed the presence of aromatic, ester, and hydroxyl functional groups on the ROFA surface after the treatment while XRD examination confirmed its carbonaceous and amorphous nature. pH 5 was found optimum for the adsorption studies at which the removal efficiencies were >71% for Cu (II) and >80% for Pb (II), while the concentration was 25 ppm for both metals. The Langmuir isotherm model was found statistically significant for both Cu (II) ($R^2 > 0.95$) and Pb (II) ($R^2 > 0.99$). ROFA has been successfully recycled in this work and the activated carbons might be considered for industrial applications.

Key words: Residual oil fly ash, Activated carbon, CO_2 activation, Steam activation, Fly ash, Physical activation.

INTRODUCTION

Residual oil fly ash (ROFA) is a by-product of the combustion process of residual fuel oil (RFO). RFO is the major fuel in Saudi Arabia which contributes to more than 70% of national energy production (ECRA, 2009). Since the ROFA generation rate is much higher in industrial cities of Saudi Arabia, its safe disposal has become a pressing concern to the authorities here. Nevertheless, ROFA possesses a great portion of unburned carbon (64-97%) based on particulate matter (PM) fractions (Huffman *et al.*, 2000). This high content of carbonaceous matter could be the perfect precursor of activated carbons which only needs an activation step (Danish *et al.*, 2013).

Activated carbons are basically porous carbon materials which have been proven as excellent adsorbents especially with attributes like high surface area and well developed pore volume, thermo-stability, chemical inertness, and adsorptive capacity (Kong *et al.*, 2013; Liu *et al.*, 2013). The recent trend in activated carbon research has been focused towards the starting or parent material which dictates the economic feasibility of the overall project (Balsamo *et al.*, 2013; Ali *et al.*, 2012; Ali, 2010). In this regard, non-conventional industrial residues such as ROFA could be of great advantage.

There are mainly two methods for activating unburned carbon from fly ash such as physical or thermal activation and chemical activation. Physical activation includes the use of either carbon dioxide (CO_2) or steam/water vapor at higher temperatures (700-1100 ^{0}C) (Sekirifa *et al.*, 2013). In chemical activation, potassium hydroxide (KOH), phosphoric acid (H_3PO_4), zinc chloride ($ZnCl_2$) etc. are used as activating agents (Davini, 2002). But some researchers recently adopted a combination of chemical and CO_2 physical activation method which is also known as

*Corresponding author E-mail: sirajussalehin@yahoo.com

physico-chemical activation. It showed better performance in adsorption capacity than commercially available activated carbons in some cases (Purnomo *et al.*, 2011, 2012).

Activated carbons with high surface areas have huge demands in industries for their excellent adsorptive capacities (Lu *et al.*, 2008). Thus, the purpose of carbon characterization is to identify and study the features of activated carbons as an end-product as well as the optimum activation operations based on different methods (Davini, 2002). The experimental procedures of carbon characterization include mainly the determination of surface areas, porous or textural properties, chemical property analysis, acidic and basic surface properties etc.

On the other hand, many industrial activities discharge effluents with heavy metals which pollute the water drastically. Heavy metals are non-biodegradable chemical elements. It mixes up with the food chain and is responsible for bioaccumulation. Over doses of copper creates gastrointestinal problems while being accumulated in liver and consequences of lead poisoning could be as serious as nervous failure (Imamoglu and Tekir, 2008). Although there are several techniques available to remove heavy metals from aqueous solutions, adsorption is the most widely used one due to its high effectiveness, low operational cost, and universality (Ali, 2014; Ali, 2012; Ali and Gupta, 2006, Rao *et al.*, 2006). Recent examples of such studies include the adsorption of lead (II), copper (II), zinc (II), nickel (II), cadmium (II), chromium (VI), and arsenic in both transitional forms (III, V) using a variety of adsorbents rather than activated carbon where the authors have reinforced the applicability of this technique (Ileri *et al.*, 2014; Amer *et al.*, 2014; Abd El fatah and Ossman, 2014; Amiri *et al.*, 2014; Andjelkovic *et al.*, 2014).

Therefore, from a waste management point of view, this study made an effort to recycle the ROFA volume in order to prepare activated carbon by physical activation methods which could be used as adsorbents of heavy metals in industries.

MATERIALS & METHODS

Residual oil fly ash (ROFA) sample was provided by Rabeigh power plant in Rabeigh, Saudi Arabia. Initially, acid leaching with 1M HCl solution was conducted to the selected samples in room temperature where the solid-liquid ratio was 1:20 (g/ml) and the mixing duration was 17 hours. Then the solution was filtered and washed several times with de-ionized water. This was done to remove the metal contents from the samples (detailed study was done separately), and to get concentrated carbon for the experiment. After that, the samples were dried in oven at 105 ^{0}C for 24 hours and kept in the desiccator prior to activation.

Samples were activated in two different ways i.e. using steam, and a mixture of steam and CO_2 gas as activating agents in a horizontal tube furnace (GSL-1800S60, MTI Inc.). The activation temperature was set at 950 ^{0}C for steam and 850 for the combined flow of gases and kept for 2 hours. Around 5 grams of sample was put in a crucible and then placed inside the tube. A raw (un-activated) ash sample was also considered for this study to compare the changes occurred due to these physical activation methods. The furnace heating rate and CO_2 pressure were maintained at 5 ^{0}C min^{-1} and 6 psi, respectively.

Multipoint BET surface area measurements were performed to get an overview of the porous characteristics of the activated samples such as surface area, and pore volume. N_2 adsorption isotherms were produced at 77 K for this purpose using Quantachrome Surface Area Analyzer equipment, NOVA 2200e. FTIR spectroscopy was employed to the samples before and after activation to determine the presence or absence of certain chemical functional groups on the activated sample surface. Transmission mode was chosen for the FTIR spectra with a frequency range between 4000-500 cm^{-1} with the aid of Bruker Alpha-E spectrometer. SEM technique was used to observe the qualitative features and the surface topography of studied samples at various magnifications using JEOL scanning electron microscope (JSM-6360 LV). XRD spectroscopy method was applied to determine the crystalline phases or textures of the studied samples. Rigaku (Ultima IV) multipurpose X-ray diffractometer was used for this purpose. XRD profile of the activated sample was achieved using Bragg's equation (Lu *et al.*, 2008) at 2θ range from 20^0 to 80^0. Batch adsorption experiments were conducted on synthetic solutions of Cu (II) and Pb (II) by using standard salts of $CuCl_2.2H_2O$ and $Pb(NO_3)_2$. Effects of initial pH (3-7), and metal concentrations (10, 25, 50, 75, 100 ppm) were examined throughout the entire study while the adsorbent dose was invariant (0.5 g/l) at all times. It needs to be mentioned that the batch adsorption experiment was designed and conducted up to 4 hours but after first 60 minutes, no change in adsorption behavior was noticed. Hence, all the adsorption experiments were performed up to 1 hour.

Erlenmeyer flasks of 250 ml were used for all the experiments and put on a magnetic stirrer. Samples were taken in different time intervals up to 60 minutes. At each time interval, 5 ml of samples was taken using standard calibrated pipette, filtered immediately, and then the filtrate was diluted up to 50 ml. Then the remaining Cu (II) and Pb (II) ions in the solutions were

analyzed by UV-Visible spectrophotometer (HACH, Lange DR6000). Chemical complex agents were used for each analysis such as LCK-(306) for Pb (II) at 520 nm and powder pillows with bicinchoninate method for Cu (II) at 560 nm.

The removal efficiency was calculated using the following formula (Imamoglu and Tekir, 2008):

$$\% \text{ Removal} = \frac{Co - Ce}{Co} \times 100 \quad (1)$$

Where, C_0 and C_e denote the initial and equilibrium concentrations of the adsorbates, individually.

For all dilutions, de-ionized water was used (Millipore, Elix) and the pH was adjusted using 0.1M solutions of HCl and NaOH.

RESULTS & DISCUSSION

BET analysis was performed and the specific surface area values were 110.89 m^2/g for raw ash, 275.07 for steam activated ash, and 423.09 for the combined steam and CO_2 activated ash. The increase in surface area was approximately 2.5 times more due to steam activation and 3.8 times higher in the samples which received the mixed flow of gases. In addition, the micropore volumes in both the activated samples (from 0.043 cc/g to 0.325 in steam activated samples and 0.078 in mixed gas flow activated samples) were broadened during the treatment (Table 1). The prepared activated carbon samples have got both micropores (< 2 nm) and mesopores (2-50 nm) that are classified by International Union of Pure and Applied Chemistry (IUPAC) (Marsh and Rodriguez-Reinoso, 2006). But, the micropore volume was found greater than the mesopore volume which resembles the findings of a recent study (Angin *et al.*, 2013).

However, some previous works regarding the surface area analysis of raw ash and activated carbons from various fly ash sources are listed in Table 2. It is seen that chemical and physico-chemical activation produced activated carbons with the highest surface areas where the sample came from agricultural sources i.e. bagasse fly ash (Purnomo *et al.*, 2011, 2012). Physical activation with either steam or carbon dioxide developed surface areas that are similar to this study (Seggiani *et al.*, 2005; Izquierdo and Rubio, 2008) and even lower (Lu *et al.*, 2008) while two different studies found much higher surface areas using the same activation method (Davini, 2002; Maroto-Valer *et al.*, 2008). Raw fly ash samples in another study (Hsieh and Tsai, 2003) showed a very lower surface area which ranged between 16-33 m^2/g. It implies that the efficiency of activated carbons in terms of surface area also depends on the sources of the samples. Figs. 1, 2 and 3 show the adsorption/desorption isotherms of nitrogen at 77 K for raw ash, steam activated ash, and combined steam and carbon dioxide activated ash, respectively. It seems that the raw ash isotherm belongs to type III of IUPAC classifications of isotherms due to its convex and upward looking nature. It indicates the adsorption of nitrogen took place at sites of poor adsorption potentials (Marsh and Rodriguez-Reinoso, 2006) and that explains the reason of showing comparatively lower surface area value.

Figs. 2 and 3 depict that adsorption took place in mesoporosity level instead of open surfaces at high relative pressure range (gas phase) which perfectly

Table 1. BET surface area and pore volume obtained from studied ROFA samples.

Samples	Experimental conditions	Surface area (m^2/g)	Pore volume (cc/g)	
			Micropore (< 2 nm)	Mesopore (2-50 nm)
RA	None	110.89	0.043	None
SA	(950 ^{0}C/2 hours)	275.07	0.325	0.088
SCA	(850 ^{0}C/2 hours)	423.09	0.078	0.028

[RA=Raw Ash; SA=Steam Activated Ash; SCA=(Steam+CO_2) Activated Ash].

Table 2. Surface area obtained in previous experiments using various fly ash sources.

Methods of Activation	Sample	Activation Agent	Carbonization Temperature (^{0}C)	Obtained Surface Area (m^2/g)	Reference
No Activation	OFA	----	----	16-33	Hsieh and Tsai, (2003)
	OFA	CO_2	850-900	1000	Davini, (2002)
Physical Activation	FA	Steam	850	1075	Maroto-Valer *et al.*, (2008)
	HOFA	CO_2	900	270	Seggiani *et al.*, (2005)
	CFA	Steam	900	416	Izquierdo and Rubio, (2008)
	CFA	Steam	850	153	Lu *et al.*, (2008)
Chemical Activation	BFA	KOH	700	2571	Purnomo *et al.*, (2012)
Physico-chemical Activation	BFA	CO_2 + $ZnCl_2$	600	1200	Purnomo *et al.*, (2011)

[FA=Fly Ash; OFA=Oil Fly Ash; HOFA=Heavy Oil Fly Ash; BFA=Bagasse Fly Ash; CFA=Coal Fly Ash].

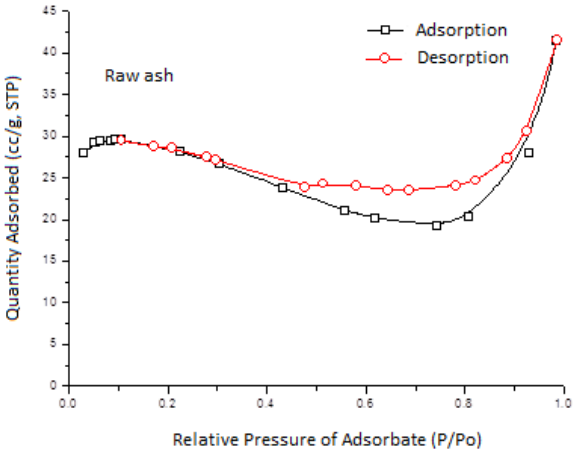

Fig. 1. N_2 adsorption/desorption isotherm of raw ROFA sample.

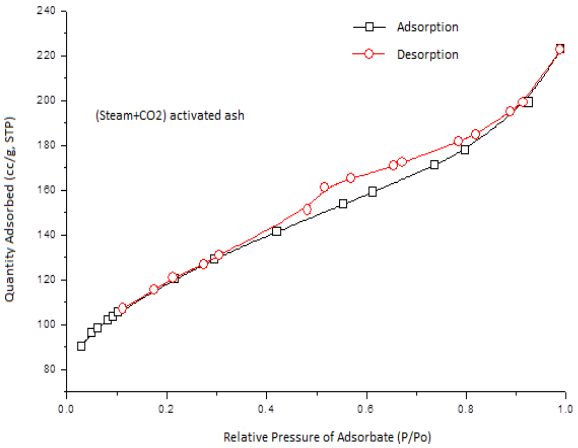

Fig. 3. N_2 adsorption/desorption isotherm of ROFA sample after combined steam and CO_2 activation.

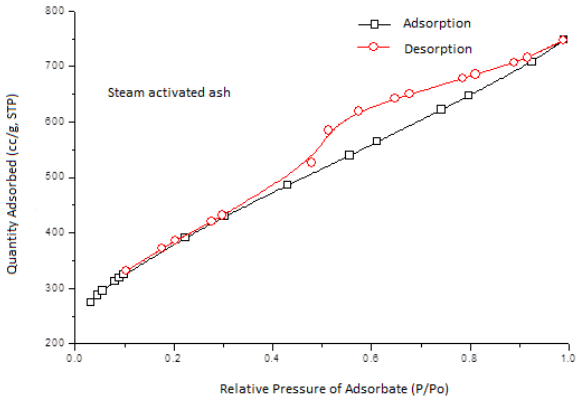

Fig. 2. N_2 adsorption/desorption isotherm of ROFA sample after steam activation.

corresponds to IUPAC isotherm type IV. The nascence of mesoporosity during activation is confirmed by the hysteresis loops as shown in Figs. 2 and 3. These loops occur when the mechanism of mesopore filling by capillary condensation varies from mesopore emptying. Besides, activated carbons generally do not show a plateau in high relative pressure region such as closer to 1 (Marsh and Rodriguez-Reinoso, 2006).

The studied ROFA samples were investigated with scanning electron microscopy to find out the morphological features of the raw ash and changes done during the activation processes. Both the raw ash and activated carbon samples were black and powdery that corresponds with earlier studies (Hsieh and Tsai, 2003). SEM micrographs of studied samples are shown in Fig. 4(a-f) where the samples appeared as cenospheres (Fig. 4a, c, and e) (Hsieh and Tsai, 2003; Seggiani *et al.*, 2005) or porous globular particles (Shawabkeh *et al.*, 2011; Yaumi *et al.*, 2013) (Fig. 4b, d, and f). The particle size ranged from very minute to as high as 100 micrometers that is relevant to another study (Shawabkeh *et al.*, 2011). The presence of various broken particles is also noticeable. Fig. 4(a-b) depicts the raw sample (before activation) with two different magnifications. It is seen that the raw sample possessed a jagged surface structure (Fig. 4b).

Steam activation brought an arranged porous network in the ash particles with developing quite smooth outer surface (Fig. 4d). Such kind of appearance was mentioned in a previous study (Hsieh and Tsai, 2003). On the other hand, the combined activation treatment increased the surface area of the raw ash quite enormously with well-developed and opened pore structures (Fig. 4f). From the morphological presentations of the samples, it can be inferred that the applied gasification changed the porous structures of the raw ash sample which finally resulted in the increased surface area and pore volume.

FTIR spectra of raw, steam activated, and mixed gas flow activated ash samples are shown in Fig. 5. In the raw ash sample, the only noticeable peak was found at 1746 cm^{-1} which was due to diketones (C=O) and was reported in several studies at different ranges such as at 1760, 1720 (Shawabkeh *et al.*, 2011; Rambabu *et al.*, 2013) and 1623 cm^{-1} (Yaumi *et al.*, 2013). Besides this, there were several minor peaks observed in the region of 596-513 cm^{-1}. The peaks closer to 560 cm^{-1} indicate the existence of Al in aluminosillicates like mullite which was reported elsewhere (Balsamo *et al.*, 2013) whereas the peaks near 516 cm^{-1} show the presence of C-C group of alkane (Patnukao *et al.*, 2008). On the other hand, steam activated sample shows extremely minor undulations at several regions such as 562-516, 1568-1470, 1694-1651, 1731-1714, and 3687-3607 cm^{-1}. The peak at 1504 cm^{-1} actually depicts the functional group of aromatic C=C which was found at

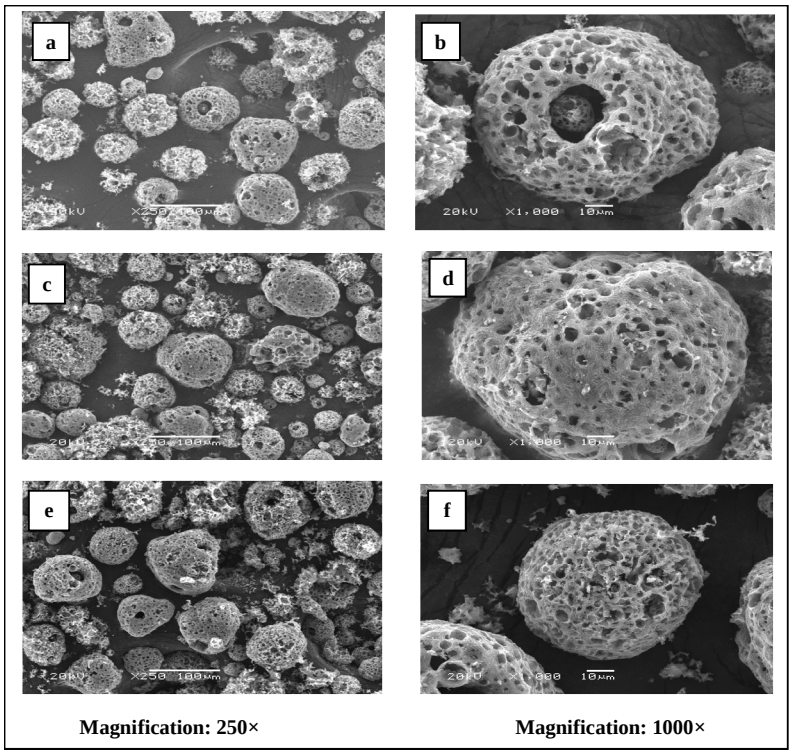

Fig. 4. SEM micrographs of studied ROFA samples: (a-b) raw ash; (c-d) steam activated ash (950 ^{0}C/2 hours); (e-f) [steam+CO_2] activated ash (850 ^{0}C/2 hours).

1467 cm^{-1} by Shawabkeh *et al.,* (2011). The peak at 3687 cm^{-1} is possibly because of stretched –O–H bond and was mentioned in previous studies where the authors observed this peak at 3650 cm^{-1} (Jiang *et al.,* 2008; Shawabkeh *et al.,* 2011). The presence of C=O which is in the ester group was found in the region of 1731-1650 cm^{-1} that was cited in a study in the range of 1760-1720 cm^{-1} (Shawabkeh *et al.,* 2011).

Nonetheless, the activated carbon prepared by mixed flow demonstrates minor peaks (613-505 cm^{-1}) similar to the raw ash sample. In addition, it has several quite detectable peaks at 950, 1504, 1789, and in between 3850 to 3687 cm^{-1} range. The peak at 950 cm^{-1} indicates the presence of C–O which was found at 1097 cm^{-1} in a previous study (Yaumi *et al.,* 2013). Therefore, it can be concluded that the surface of activated carbon samples showed aromatic, ester, and hydroxyl functional groups on their surface.

XRD patterns of the raw, steam activated, and mixed steam and CO_2 activated ash samples are illustrated in Fig. 6. In all the samples, similar type of broad peaks evolved which were reflected from the planes. These broad peaks reveal the highly disordered and amorphous nature of raw ash and activated carbons that were dealt with in this experiment. This behavior might be due to the acid treatment that was discussed before which completely removed the sharp peaks associated with the ash (Lu *et al.,* 2008). In general, the alike broad diffractions in every sample match with graphitic reflections near 26^0=2θ and it suggests a particular graphitic array in the molecular planes along with the presence of mullite which was mentioned in previous studies (Danish *et al.,* 2013; Yaumi *et al.,* 2013). In addition, minor broad peaks were also seen closer to 43^0=2θ which indicates the existence of mullite or sodalite (Shawabkeh *et al.,* 2011).

However, the interlayer space (d) varied from 3.474-3.511 A^0 in studied samples which were larger than the graphite (3.354 A^0). It implies all the prepared samples had carbonaceous structure (Kong *et al.,* 2013). Besides, the negligibility of crystalline phases in the samples fits in with porous nature of the studied samples which were again supported by SEM study and this phenomenon was described elsewhere (Al-Degs *et al.,* 2014).

The effect of initial pH of the solution on adsorption is very dynamic as it is directly involved in altering the surface charge of the adsorbent (Givianrad *et al.,* 2013; Imamoglu and Tekir, 2008) which could be influential in determining the adsorption efficiency. Therefore, five different pH ranges (3-7) were studied to select the optimum one that could adsorb the two heavy metals of interest at the highest level. Fig. 7 depicts the rate of adsorption with increasing pH levels.

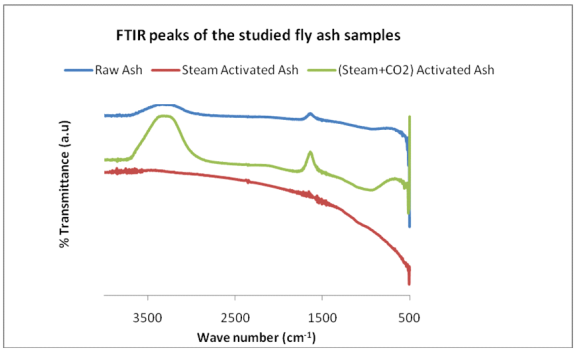

Fig. 5. FTIR spectra of studied ROFA samples.

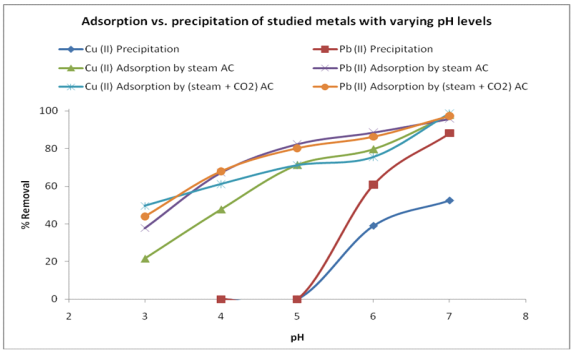

Fig. 7. Effect of initial pH on Cu (II) and Pb (II) adsorption (adsorbent dose 0.5 g/l, contact time 60 minutes, initial metals concentration 25 ppm).

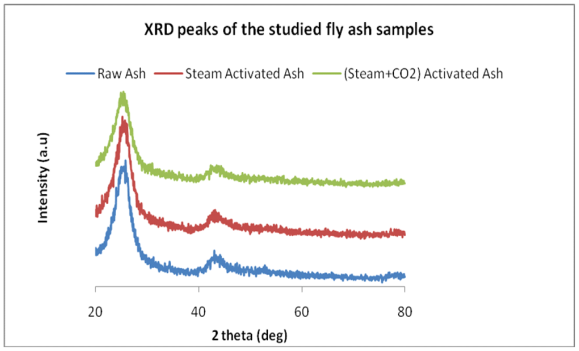

Fig. 6. XRD patterns of studied ROFA samples.

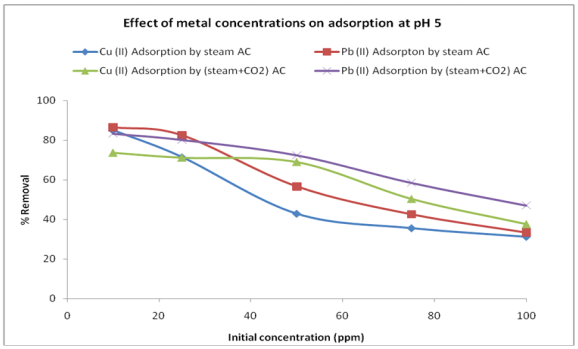

Fig. 8. Effect of metal concentrations on Cu (II) and Pb (II) adsorption (adsorbent dose 0.5 g/l, pH 5, contact time 60 minutes).

The adsorption efficiency values with different pH levels were 21.7, 47.8, 71.4, 79.8, and 98% for Cu (II); 37.8, 67.3, 82.4, 88.6, and 95.9% for Pb (II) in steam activated samples at pH 3, 4, 5, 6, and 7, respectively. The removal rates in combined gasification activated samples were 49.6, 61.2, 71.2, 75.6, and 98.8% for Cu (II) whereas 44, 68, 80.2, 86.3, and 97.4% were found for Pb (II) with same pH order mentioned above.

For both metals, the adsorption efficiency increased with the increase of the initial pH. Reduced adsorption phenomena were observed at lower pH levels such as 3 and 4 for both metals. This is due to the protonation that occurs at the active sites of the adsorbent which restricts the spontaneous uptake of the metal ions present in the solution (Cechinel *et al.*, 2013; Givianrad *et al.*, 2013; Patnukao *et al.*, 2008). Higher removal rates of Cu (II) and Pb (II) were achieved at pH 6 and 7. Usually, precipitation of these two metals takes place at those pH levels as insoluble metal hydroxides, thus the metal removal at such pH is a combination between precipitation and adsorption (Cechinel *et al.*, 2013; Imamoglu and Tekir, 2008). For this, a separate experiment was conducted to find out the precipitation behavior of the studied metals under the current experimental conditions. That experiment revealed that both the Cu (II) and Pb (II) ions did not precipitate until pH 5. But at pH 6 and 7, both the metals precipitated to a significant level (Fig. 7). Hence, pH 5 was considered as the optimum pH for adsorption of the studied metals in this experiment and used for later experiments.

The effect of metal concentrations on the adsorption efficiency of Cu (II) and Pb (II) is presented in Fig. 8. It is clear that the percentage of adsorption increased as the initial metals concentrations were decreased. The adsorption efficiency values were 85, 71.4, 42.9, 35.5, and 31.2% for Cu (II) while the values were 86.5, 82.4, 56.7, 42.6, and 33.3% for Pb (II) in steam activated samples with initial metals concentration of 10, 25, 50, 75, and 100 ppm, respectively. And in mixed gasification activated samples, the efficiency rates were 73.7, 71.2, 68.9, 50.3, and 37.5% for Cu (II); 83.4, 80.2, 72.5, 58.5, and 47% for Pb (II) for the concentrations of same orders mentioned above.

A previous study mentioned about enough vacant adsorption sites at lower metals concentrations whereas at higher concentrations, the number of metal ions become abundant than the adsorption sites and

Table 3. Values of Langmuir and Freundlich constants for Cu (II) and Pb (II) adsorption isotherms.

Studied AC types and adsorbates		Langmuir constants			Freundlich constants		
		K_L (L/mg)	q_m (mg/g)	R^2 (corr.coeff.)	K_F [mg/g(L/mg)$^{1/n}$]	n	R^2 (corr. coeff.)
SA	Cu (II)	0.159	52.63	0.9694	13.95	3.17	0.9553
	Pb (II)	0.293	56.81	0.9991	16.65	3.09	0.9003
SCA	Cu (II)	0.135	64.52	0.9533	10.46	2.02	0.7837
	Pb (II)	0.187	80	0.9952	14.02	2.01	0.8953

[SA=Steam Activated Ash; SCA=(Steam+CO_2) Activated Ash].

Table 4. Linear Dubinin-Radushkevich isotherm parameters.

Adsorbents	Studied metals	q_{DR} (mg/g)	B_{DR} (mmol^2/J^2)	E (kj/mol)	R^2 (corr. coeff.)
SA	Cu (II)	39.35	5E - 07	1	0.8649
	Pb (II)	47.66	5E - 07	1	0.9472
SCA	Cu (II)	48.35	1E - 06	0.71	0.9326
	Pb (II)	60.35	8E - 07	0.79	0.952

[SA=Steam Activated Ash; SCA=(Steam+CO_2) Activated Ash]

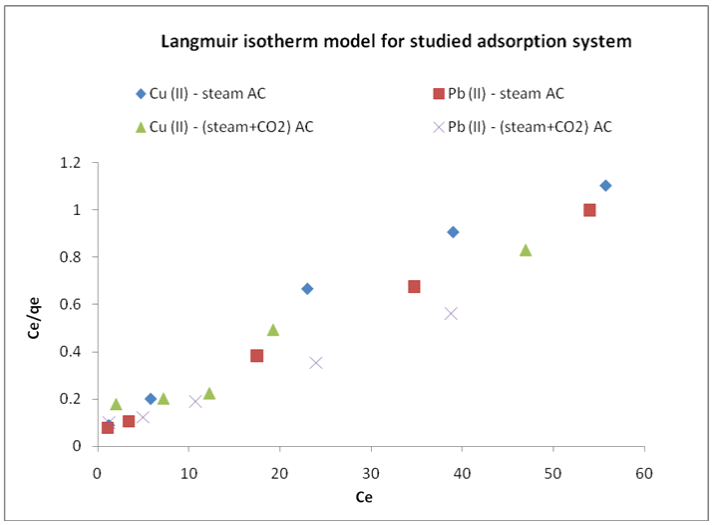

Fig. 9. Langmuir isotherm model for Pb (II) and Cu (II) adsorption.

hence the reduced adsorption efficiency (Imamoglu and Tekir, 2008). Therefore, it could be inferred that the adsorption of both Cu (II) and Pb (II) was extremely concentration reliant and with lower initial concentrations, Pb (II) could be removed more efficiently than Cu (II). In any adsorption system, adsorption isotherms are of immense importance to find out the correlations between adsorbate and adsorbent at equilibrium conditions. There are several models with distinguished parameters which facilitate to understand the adsorption mechanism, behavior of the adsorbent surface during adsorption and its capacity to adsorb in certain experimental circumstances upon the fitness to each of these models (Oladipo and Gazi, 2014; Kong *et al.*, 2013). This study investigated two adsorption isotherm models that are widely used: Langmuir (Eq. (2)) and Freundlich (Eq. (3)) models (Cechinel *et al.*, 2013):

$$\frac{Ce}{qe} = \frac{1}{KL.qm} + \frac{Ce}{qm} \quad (2)$$

$$lnqe = lnKF + \frac{1}{n}.lnCe \quad (3)$$

For Langmuir model, 'K_L' is the Langmuir constant for adsorption (L/mg); 'q_m' indicates theoretical maximum adsorption capacity (mg/g).

In the other model, 'K_F' represents the Freundlich constant of adsorption capacity [mg/g (L/mg)$^{1/n}$]; 'n' denotes the favorability of adsorption process or adsorption intensity in other words (Kong *et al.*, 2013). The calculated parameters of both Langmuir and Freundlich models are presented in Table 3.

It is clearly seen that the studied adsorption process fitted well with the Langmuir model (Fig. 9) due to the highest correlation coefficient (R^2) values

for Cu (II) and Pb (II) which were 0.97 and 0.99 in steam activated samples and 0.95 and 0.99 in combined gas activated samples, respectively. It implies that the adsorption occurred in a monolayer and there was homogenous distribution of active adsorption sites on both activated carbon samples (Kong *et al.*, 2013; Bulut and Tez, 2007). Cechinel *et al.*, (2013) also added a feature to this model that all the active adsorption sites have same attraction to the adsorbate molecules.

Dubinin-Radushkevich model is an empirical isotherm model which was conceptualized for adsorbing subcritical vapors onto micropore adsorbents that follows a pore filling mechanism. This model describes the adsorption mechanism with a Gaussian energy distribution onto a heterogeneous surface. This model is used to differentiate the physisorption or chemisorption of metal ions on the adsorbent surface, by calculating the value of mean free energy for per molecule of adsorbate, *E* (kJ/mole) with the following equation:

$$E = \left[\frac{1}{\sqrt{2B_{DR}}}\right] \quad (4)$$

Where, B_{DR} denotes the isotherm constant. If the value of E is less than 1 to 8 kJ mol^{-1}: it is considered to be a physical adsorption mechanism; while the value between 8 to 16 kJ mol^{-1} indicates the occurrence of ion-exchange; and if the range is between 20 to 40 kJ mol^{-1} then it is an indicative of chemical adsorption on the adsorbent (Kazmi *et al.*, 2012; Ho *et al.*, 2002).

There is another parameter called the Polanyi potential, ε (J $mmol^{-1}$) which can be calculated as:

$$\varepsilon = RT \ln\left[1 + \frac{1}{C_e}\right] \quad (5)$$

Where, R indicates the universal gas constant (8.314 J mol^{-1} K^{-1}), T represents the absolute temperature (in Kelvin), and C_e to equilibrium concentration of adsorbate (mg/L). The unparalleled feature of this isotherm model is it is temperature dependent. When adsorption data with different temperatures are plotted, it produces the '*characteristic curve*' (Foo and Hameed, 2010).

The linearized equation of D-R isotherm model is:

$$\ln q_e = \ln q_{DR} - B_{DR} \times \varepsilon^2 \quad (6)$$

Where, q_{DR} indicates the saturation capacity of the adsorbent. The plot was drawn as ln q_e vs. ε^2 and all the calculated parameters are shown in Table 4.

It is seen that, all the experimental E value ranged between 0.71-1, which clearly demonstrates the physical adsorption of both Cu (II) and Pb (II) ions onto the prepared activated carbons. These results are in well conformity with the FTIR analysis of the AC samples, where not much chemical functional groups were found before and after the treatment. Therefore, it was not expected that chemisorption would take place for the studied metals with these adsorbents and the D-R isotherm model proves it very well.

This D-R isotherm model for this experiment is graphically represented in Fig. 10.

CONCLUSIONS

Activated carbons were prepared successfully from ROFA by physical activation methods using either steam or a combination of steam and CO_2 at 850-950 ^{0}C with a holding time of 2 hours. The BET surface area increased during both activation methods; but the combined flow of gases showed better surface area

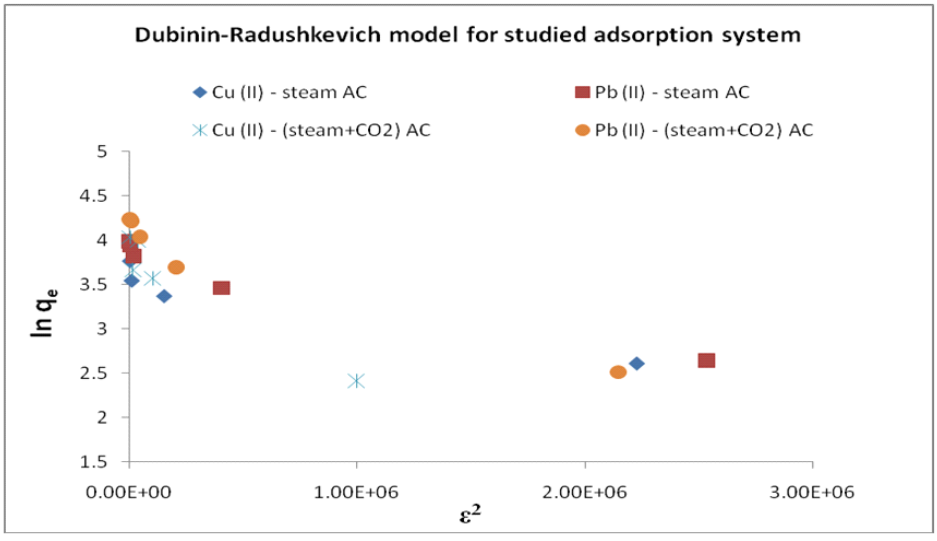

Fig. 10. Dubinin-Radushkevich isotherm model for Cu (II) and Pb (II) adsorption.

(423.09 m^2/g) than the single steam flow (275.07 m^2/g) where the surface area of raw ash was quite lower (110.89 m^2/g). SEM analysis showed that both the gasification treatments on raw fly ash sample changed the porous structure and network which resulted in higher surface areas in the activated samples. FTIR spectroscopic examination revealed the attachments of new functional groups of aromatic, ester, hydroxyl compounds on the surface of activated carbons. XRD results confirm the amorphous nature of ROFA volume with the presence of broad peaks near 26^0 at 2-theta angle. At optimum pH level 5, >71% of Cu (II) and >80% of Pb (II) ions were removed from synthetic aqueous solutions. Study on various metal concentrations showed that the activated carbons were more effective with lower concentrations. The experimental adsorption data followed the Langmuir isotherm model which demonstrates the occurrence of adsorption in a monolayer with homogenous active adsorption sites on the surface of the adsorbents. The recycling of ROFA has been successful in this study and the activated carbons may be used for industrial applications of metal adsorption.

ACKNOWLEDGEMENTS

The authors sincerely acknowledge King Abdulaziz City for Science and Technology (KACST) (Project: 8-ENV124-3) for funding this study.

REFERENCES

Abd El fatah, M. and Ossman, M.E. (2014). Removal of Heavy Metal by Nickel Oxide Nano Powder. Int. J. Environ. Res., **8**, 741-750.

Al-Degs, Y. S., Ghrir, A., Khoury, H., Walker, G. M., Sunjuk, M. and Al-Ghouti, M. A. (2014). Characterization and utilization of fly ash of heavy fuel oil generated in power stations. Fuel Processing Technology, **123**, 41-46.

Ali, I. (2014). Water Treatment by Adsorption Columns: Evaluation at Ground Level. Sepn. & Purfn. Rev., **43**, 175-205.

Ali, I. (2012). New Generation Adsorbents for Water Treatment. Chem. Revs., **112**, 5073-5091.

Ali, I., Asim, M. and Khan, T.A. (2012). Low cost adsorbents for removal of organic pollutants from wastewater. J. Environ. Manag., **113**, 170-183.

Ali, I. (2010). The Quest for Active Carbon Adsorbent Substitutes: Inexpensive Adsorbents for Toxic Metal Ions Removal from Wastewater. Sepn. & Purfn. Rev., **39**, 95-171.

Ali, I. and Gupta, V.K. (2006). Advances in Water Treatment by Adsorption Technology. Nature Protocol, **1**, 2661-2667.

Amer, R.A., Ossman, M.E., Hassan, H.S., Ghozlan, H. and Sabry, S.A. (2014). Adsorption of Ni(II) by Exiguobacterium sp. 27 and Polyaniline Nanoparticles. Int. J. Environ. Res., **8**, 601-612.

Amiri, M.J., Fadaei, E., Baghvand, A. and Ezadkhasty, Z. (2014). Removal of Heavy Metals Cr (VI), Cd (II) and Ni (II) from Aqueous Solution by Bioabsorbtion of Elaeagnus Angustifolia. Int. J. Environ. Res., **8**, 411-420.

Andjelkovic, I., Manojlovic, D., Skrivanj, S., Pavlovic, B.M., Amaizah, N.R. and Roglic, G. (2014). As(III) and As(V) Sorption on MnO2 Synthesized by Mechano-chemical Reaction from Aqueous phase. Int. J. Environ. Res., **8**, 395-402.

Angin, D., Kose, T. E. and Selengil, U. (2013). Production and characterization of activated carbon prepared from safflower seed cake biochar and its ability to absorb reactive dyestuff. Applied Surface Science, **280**, 705-710.

Balsamo, M., Natale, F. D., Erto, A., Lancia, A., Montagnaro, F. and Santoro, L. (2013). Gasification of coal combustion ash for its reuse as adsorbent. Fuel, **106**, 147-151.

Bulut, Y. and Tez, Z. (2007). Removal of heavy metals from aqueous solution by sawdust adsorption. Journal of Environmental Sciences, **19**, 160-166.

Cechinel, M. A. P., de Souza, S. M. A. G. U. and de Souza, A. A. U. (2013). Study of lead (II) adsorption onto activated carbon originating from cow bone. Journal of Cleaner Production, 1-8.

Danish, M., Hashim, R., Ibrahim, M. N. M. and Sulaiman, O. (2013). Effect of acidic activating agents on surface area and surface functional groups of activated carbons produced from *Acacia mangium* wood. Journal of Analytical and Applied Pyrolysis, **104**, 418-425.

Davini, P. (2002). Flue gas treatment by activated carbon obtained from oil-fired fly ash. Carbon, **40**, 1973-1979.

ECRA (Electricity and Cogeneration Regularity Authority). (2009). Annual Report 2009.

Foo, K.Y. and Hameed, B.H. (2010). Insights into the modeling of adsorption isotherm systems. Chemical Engineering Journal, **156**, 2-10.

Givianrad, M. H., Rabani, M., Tehrani, M. S., Azar, P. A. and Sabzevari, M. H. (2013). Preparation and characterization of nanocomposite, silica aerogel, activated carbon and its adsorption properties for Cd (II) ions from aqueous solution. Journal of Saudi Chemical Society, **17**, 329-335.

Ho, Y.S., Porter, J.F. and Mckay, G. (2002). Equilibrium isotherm studies for the sorption of divalent metal ions onto peat: copper, nickel and lead single component systems. Water, Air, and Soil Pollution, **141**, 1-33.

Hsieh, Y. M. and Tsai, M. S. (2003). Physical and chemical analyses of unburned carbon from oil-fired fly ash. Carbon, **41**, 2317-2324.

Huffman, G. P., Huggins, F. E., Shah, N., Huggins, R., Linak, W. P., Miller, C. A., Pugmire, R. J., Meuzelaar, H. L. C., Seehra, M. S. and Mannivannan, A. (2000). Characterization of Fine Particulate Matter Produced by Combustion of

Residual Fuel Oil. Journal of the Air & Waste Management Association, **50**, 1106-1114.

Ileri, O., Cay, S., Uyanik, A., Erduran, N. (2014). Removal of Common Heavy Metals from Aqueous Solutions by Waste Salvadora persica L. Branches (Miswak). Int. J. Environ. Res., **8**, 987-996.

Imamoglu, M. and Tekir, O. (2008). Removal of copper (II) and lead (II) ions from aqueous solutions by adsorption on activated carbon from a new precursor hazelnut husks. Desalination, **228**, 108-113.

Izquierdo, M. T. and Rubio, B. (2008). Carbon-enriched coal fly ash as a precursor of activated carbons for SO_2 removal. Journal of Hazardous Materials, **155**, 199-205.

Jiang, Y., Elswick, E. R. and Mastalerz, M. (2008). Progression in sulfur isotopic compositions from coal to fly ash: examples from single-source combustion in Indiana. International Journal of Coal Geology, **73**, 273.

Kazmi, M., Feroze, N., Javed, H., Zafar, M. and Ramzan, N. (2012). Biosorption of Cu (II) on dry-fruit byproduct: characterization, kinetic and equilibrium studies. J. Chem. Soc. Pak., **34**, 1356-1365.

Kong, J., Yue, Q., Huang, L., Gao, Y., Sun, Y., Gao, B., Li, Q. and Wang, Y. (2013). Preparation, characterization and evaluation of adsorptive properties of leather waste based activated carbon via physical and chemical activation. Chemical Engineering Journal, **221**, 62-71.

Liu, D., Yuan, W., Yuan, P., Yu, W., Tan, D., Liu, H. and He, H. (2013). Physical activation of diatomite-templated carbons and its effects on the adsorption of methylene blue (MB). Applied Surface Science, **282**, 838-843.

Lu, Z., Maroto-Valer, M. M. and Schobert, H. H. (2008). Role of active sites in the steam activation of high unburned carbon fly ashes. Fuel, **87**, 2598-2605.

Maroto-Valer, M. M., Lu, Z., Zhang, Y. and Tang, Z. (2008). Sorbents for CO_2 capture from high carbon fly ashes. Waste Management, **28**, 2320-2328.

Marsh, H. and Rodriguez-Reinoso, F. (2006). Activated Carbon. Elsevier Science & Technology Books, Amsterdam, 1-420.

Oladipo, A.A. and Gazi, M. (2014). Enhanced removal of crystal violet by low cost alginate/acid activated bentonite composite beads: Optimization and modelling using non-linear regression technique. Journal of Water Process Engineering, **2**, 43-52.

Patnukao, P., Kongsuwan, A. and Pavasant, P. (2008). Batch studies of adsorption of copper and lead on activated carbon from *Eucalyptus camaldulensis Dehn*. bark. Journal of Environmental Sciences, **20**, 1028-1034.

Purnomo, C. W., Salim, C. and Hinode, H. (2011). Preparation and characterization of activated carbon from bagasse fly ash. Journal of Analytical and Applied Pyrolysis, **91**, 257-262.

Purnomo, C. W., Salim, C. and Hinode, H. (2012). Effect of the activation method on the properties and adsorption behavior of bagasse fly ash-based activated carbon. Fuel Processing Technology, **102**, 132-139.

Rambabu, N., Azargohar, R., Dalai, A. K. and Adjaye, J. (2013). Evaluation and comparison of enrichment efficiency of physical/chemical activations and functionalized activated carbons derived from fluid petroleum coke for environmental applications. Fuel Processing Technology, **106**, 501-510.

Rao, M. M., Ramesh, A., Rao, G. P. C. and Seshaiah, K. (2006). Removal of Copper and Cadmium from the Aqueous Solutions by Activated Carbon Derived from Ceiba pentandra Hulls. Journal of Hazardous Materials, **129**, 123-129.

Seggiani, M., Vitolo, S. and Filippis, P. D. (2005). Effect of pre-oxidation on the porosity development in a heavy oil fly ash by CO_2 activation. Fuel, **84**, 1854-1857.

Sekirifa, M. L., Hadj-Mahammed, M., Pallier, S., Baameur, L., Richard, D. and Al-Dujaili, A. H. (2013). Preparation and characterization of an activated carbon from a date stones variety by physical activation with carbon dioxide. Journal of Analytical and Applied Pyrolysis, **99**, 155-160.

Shawabkeh, R., Khan, M. J., Al-Juhani, A. A., Wahhab, H. I. A. A. and Hussein, I. A. (2011). Enhancement of surface properties of oil fly ash by chemical treatment. Applied Surface Science, **258**, 1643-1650.

Yaumi, A. L., Hussein, I. A. and Shawabkeh, R. A. (2013). Surface modification of oil fly ash and its application in selective capturing of carbon dioxide. Applied Surface Science, **266**, 118-125.